

Crystal structures and physicochemical properties of diltiazem base and its acetylsalicylate, nicotinate and L-malate salts

D. Stepanovs, M. Jure, M. Gosteva, J. Popelis, G. Kiselovs and A. Mishnev

Supporting Information

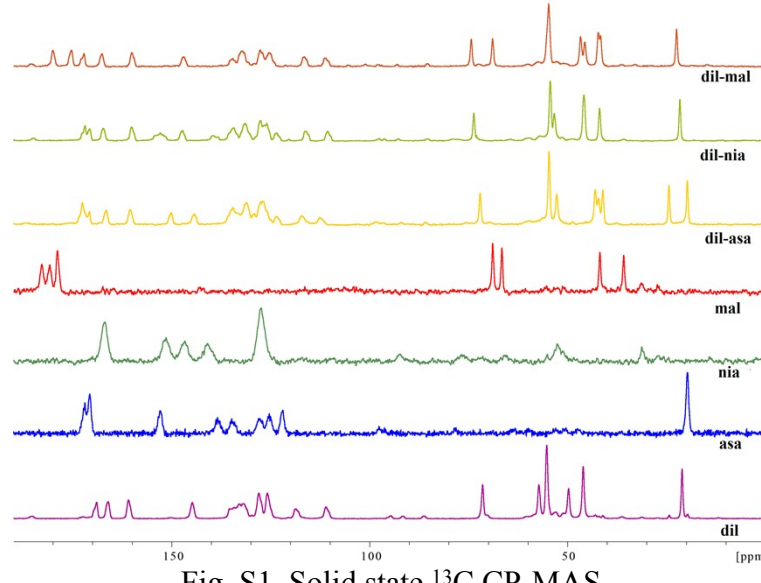


Fig. S1. Solid state ^{13}C CP-MAS

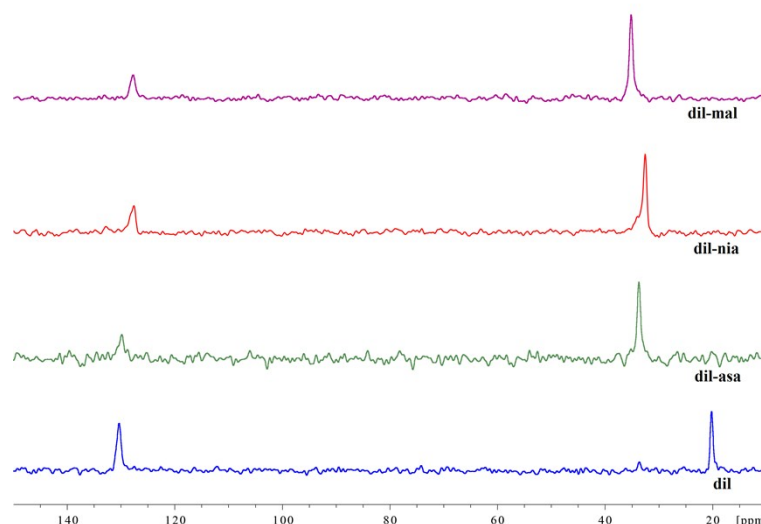
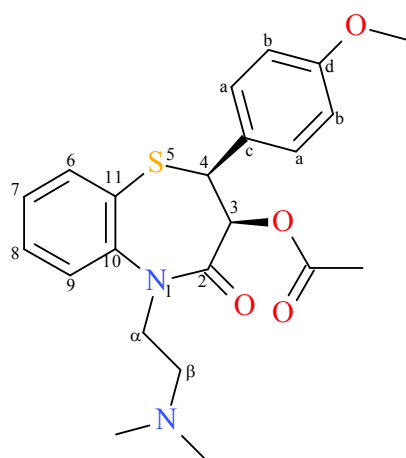


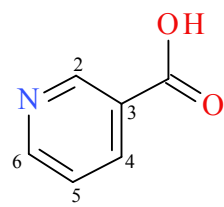
Fig. S2. Solid state ^{15}N CP-MAS

S3. NMR ^1H and ^{13}C chemical shifts for **dil** and its salts

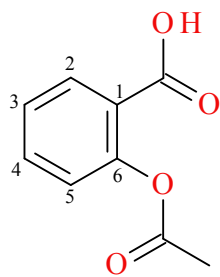
dil



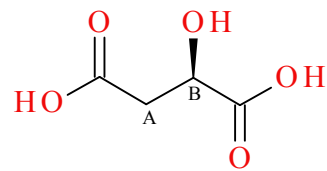
nia



asa



mal



^1H NMR chemical shifts

HSQC, dil-HCl	dil-HCl		dil	HSQC, dil	dil-nia	dil-asa	dil-mal
70.42	4.99	H-3	4.98	70.32	4.99	4.97	4.99
53.11	5.16	H-4	5.11	53.21	5.12	5.12	5.13
135.32	7.76 dd2	H-6	7.70	124.80	7.71	7.71	7.72
128.02	7.42 ddd2	H-7	7.34	127.35	7.49	7.35	7.37
131.57	7.65 ddd1	H-8	7.59	131.13	7.59	7.59	7.61
124.59	7.71 dd1	H-9	7.71	134.92	7.70	7.69	7.71
144.34	-	C-10	-	145.19	-	-	-
127.26	-	C-11	-	127.35	-	-	-
130.77	7.38	H- <i>a</i>	7.43	130.87	7.42	7.41	7.41
113.56	6.93	H- <i>b</i>	6.91	113.42	6.92	6.91	6.91
126.60	-	C- <i>c</i>	-	127.00	-	-	-
159.21	-	C- <i>d</i>	-	159.16	-	-	-
55.06	3.77	O-CH ₃	3.77	55.03	3.77	3.76	3.77
43.69	4.17 4.44	H- <i>a</i>	3.71 4.26	46.81 4,3	3.81 4.28	3.76 4.28	3.85 4.31

52.45	3.12 3,45	H- β	2.28 2.51	56.50	2.42 2.69	2.39 2.64	2.59 2.86
20,21	1.83	CH ₃ -C=O	1.82	20.24	1.82	1.82	1.82
169.24	-	CH ₃ -C=O	-	169.14			
167.06	-	C-2	-	166.17			
42.11	2.79 br	N-CH ₃	2.13	45.21	2.25	2.22	2.38

		nia		dil-nia		
	H-2	9.08		9.06		
	H-4	8.28		8.24		
	H-5	7.55		7.51		
	H-6	8.80		8.74		
	OH	13.40		...		

				asa	dil-asa	
		H-2		7.93	7.91	
		H-3		7.37	7.36	
		H-4		7.63	7061	
		H-5		7.19	7.17	
		CH ₃ C=O		2.24	2.23	
		OH		13.10	...	

					mal	dil-mal
				H-A	2.44 2.61	2.39 2.57
				H-B	4.25	4.12
				OH	12.40	...

¹³C NMR chemical shifts

dil-HCl		dil	dil-nia	dil-asa	dil-mal
167.06	C2=O	166.17	166.33	165.76	166.54
70.42	C-3	70.32	70.35	70.34	70.36
52.45	C-4	53.21	53.21	53.20	55.14
135.32	C-6	134.92	135.00	134.99	135.10
127.63	C-7	127.63	127.58	127.59	127.53
126.60	C-8	127.00	126.94	126.95	126.85
124.59	C-9	124.80	124.75	124.77	124.72
144.34	C-10	145.19	145.06	145.08	144.87
128.02	C-11	127.35	127.48	127.47	127.64
43.69	C- α	46.81	46.29	46.39	45.73
53.11	C- β	56.50	55.78	55.96	53.19

130.77	C- <i>a</i>	130.87	130.87	130.87	130.85
113.56	C- <i>b</i>	113.42	113.45	113.45	113.47
131.57	C- <i>c</i>	131.13	131.20	131.20	131.30
159.21	C- <i>d</i>	159.16	159.18	159.17	159.19
169.24	O-C=O	169.14	169.17	166.31	169.19
55.06	O-CH ₃	55.03	55.05	55.05	55.06
42.11	N-CH ₃	45.21	44.64	44.79	44.19
20.21	CH ₃ -C=O	20.24	20.24	20.25	20.24

		nia	dil-nia		
	C-2	150.22	150.24		
	C-3	126.56	127.81		
	C-4	136.94	136.80		
	C-5	123.79	123.60		
	C-6	153.28	152.69		
	C=O	166.27	166.68		

			asa	dil-asa	
		C-1	124.04	123.69	
		C-2	123.77	124.48	
		C-3	126.05	125.98	
		C-4	131.37	131.35	
		C-5	133.77	133.54	
		C-6	150.17	150.12	
		CH ₃ -C=O	20.84	20.86	
		CH ₃ -C=O	169.17	169.17	
		HO-C=O	165.60	n/a	

				mal	dil-mal
			C- <i>A</i>	39.29	44.16
			C- <i>B</i>	67.03	66.62
			C- <i>A</i> -COOH	171.84	171.91
			C- <i>B</i> -COOH	174.62	175.37

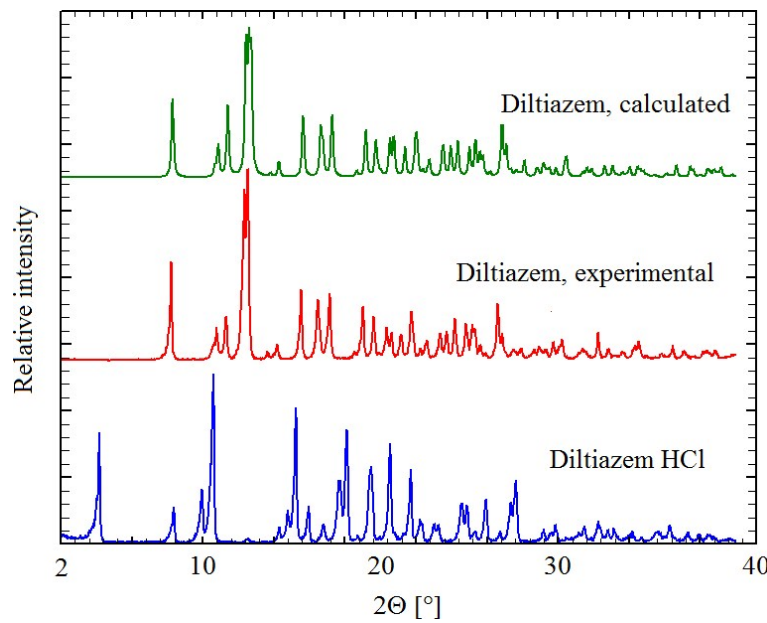


Fig. S4. Experimental PXRD pattern of diltiazem HCl (**dil-HCl**); experimental and calculated PXRD patterns of diltiazem base (**dil**)

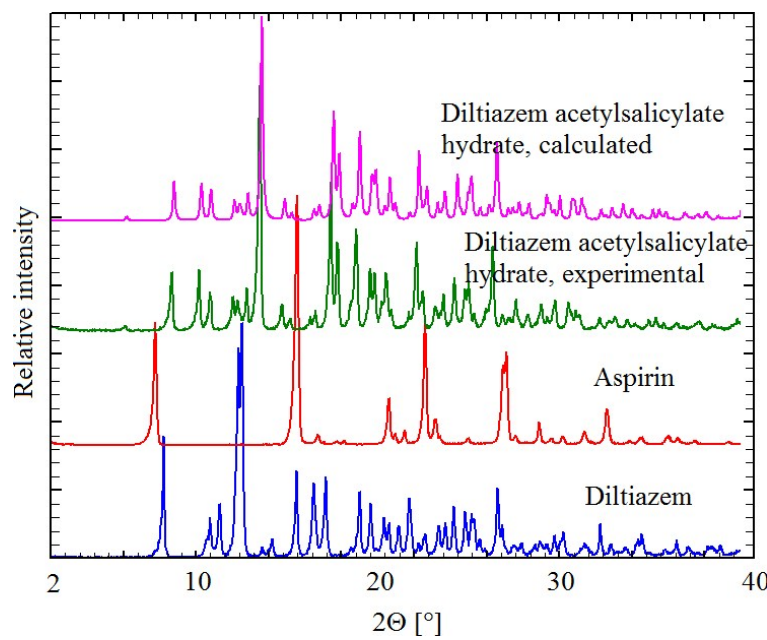


Fig. S5. Experimental PXRD patterns of diltiazem (**dil**) and aspirin (**asa**) in comparison with experimental and calculated patterns of diltiazem acetylsalicylate hydrate (**dil-asa**)

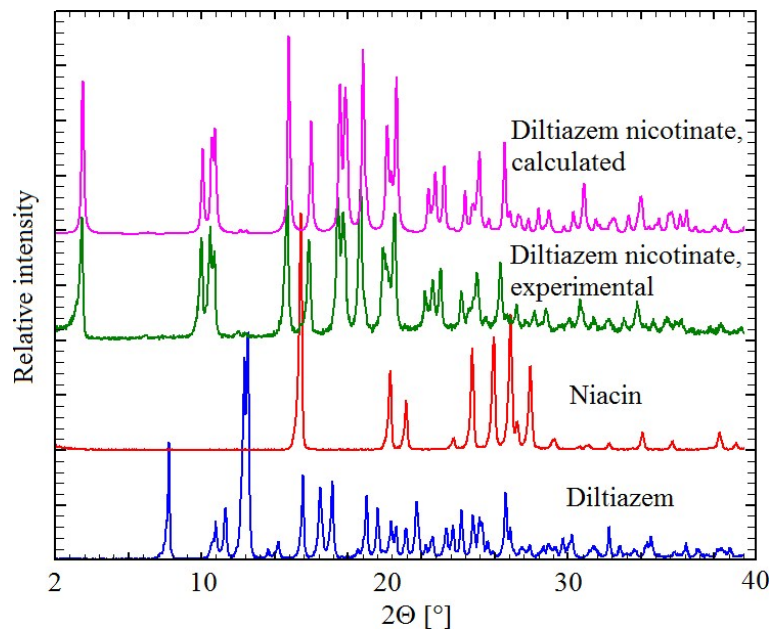


Fig. S6. Experimental PXRD patterns of diltiazem (**dil**) and Niacin (**nia**) in comparison with experimental and calculated patterns of diltiazem nicotinate (**dil-nia**)

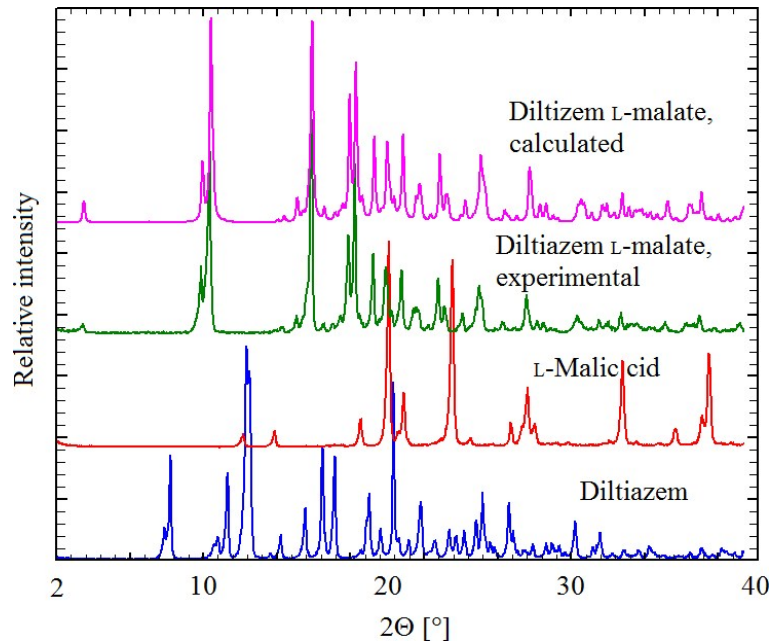


Fig. S7. Experimental PXRD patterns of diltiazem (**dil**) and L-malic (**mal**) in comparison with experimental and calculated patterns of diltiazem L-malate (**dil-mal**)

Note: The calculated¹ and experimental X-ray diffraction patterns are equivalent (Figures S1–S4) (calculated⁴⁰ patterns are shifted a little to the right along x axis, because

experimental PXRD patterns were measured at room temperature, while single crystal X-ray measurements were carried out at low temperature of 173 (2) K.

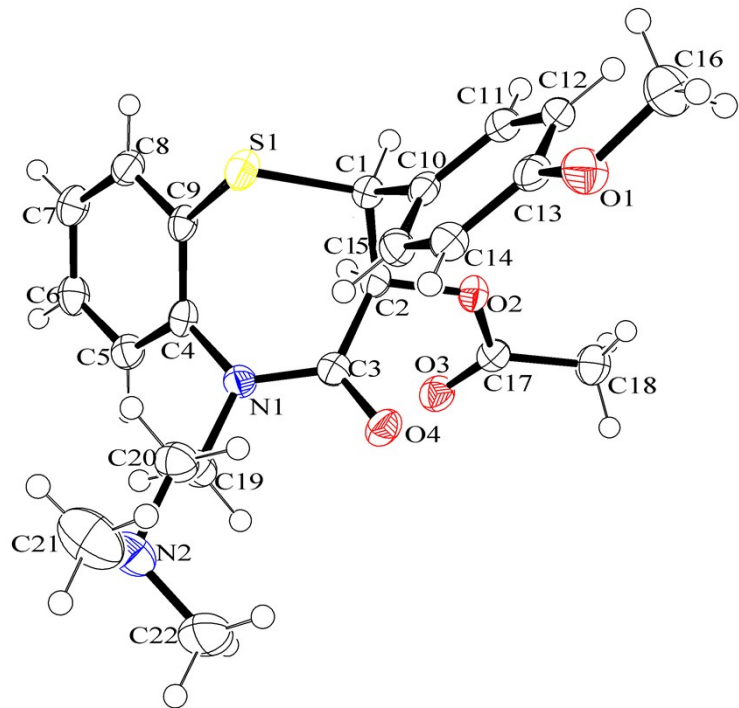


Fig. S8. ORTEP drawing of **dil**, showing the atom-numbering scheme

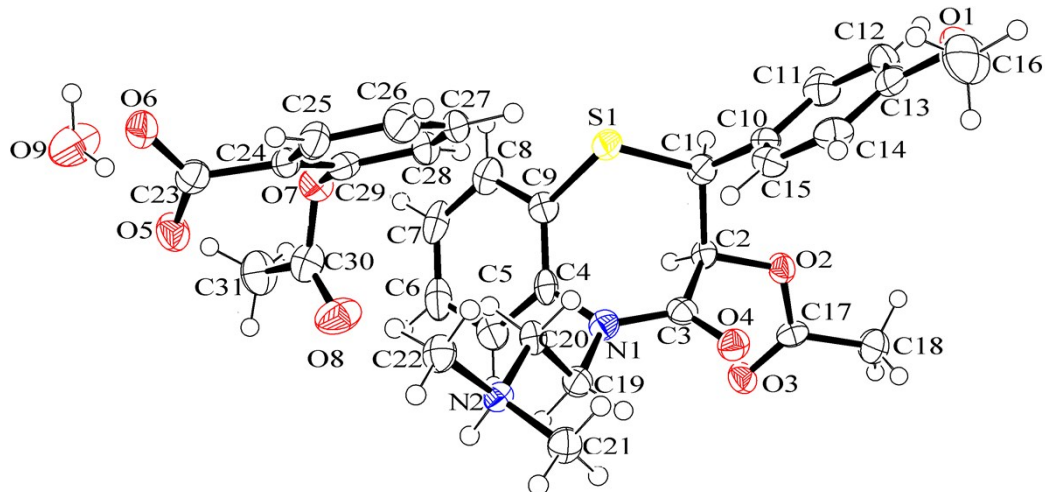


Fig. S9. ORTEP drawing of **dil-asa**, showing the atom-numbering scheme

¹ A calculated PXRD patterns were generated from the single crystal structures using Mercury CSD 31.1⁴⁰ and compared with the patterns collected from the bulk sample

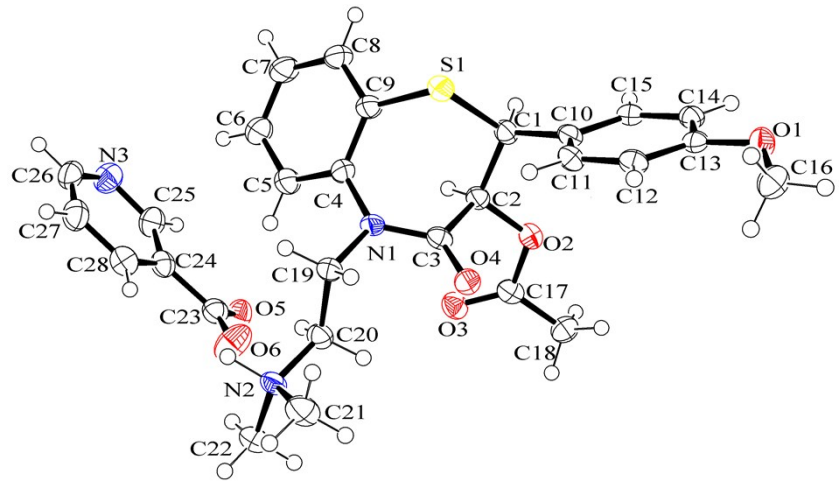


Fig. S10. ORTEP drawing of **dil-nia**, showing the atom-numbering scheme

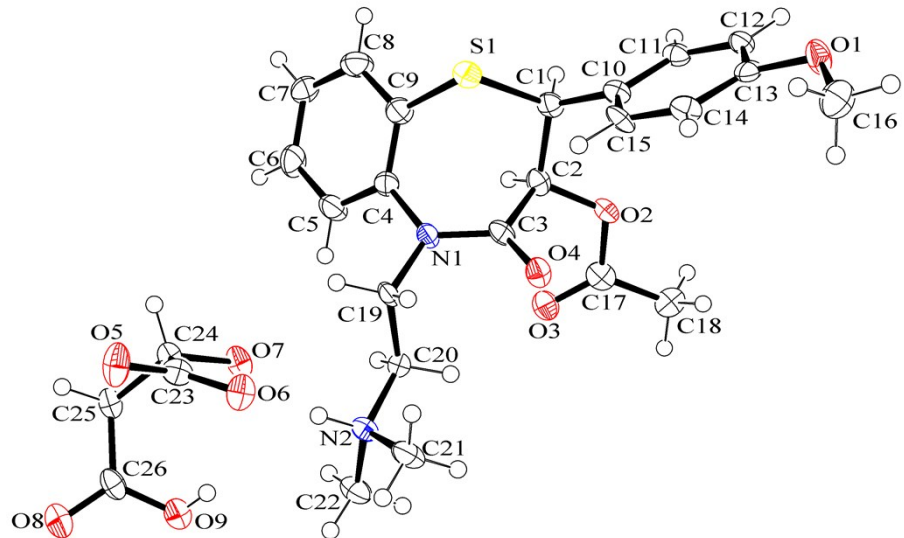


Fig. S11. ORTEP drawing of **dil-mal**, showing the atom-numbering scheme

Table S12. Torsion angles (τ) in the seven-membered ring

Compound \ τ , °	C2–S1–C1–C9	S1–C1–C2–C3	C1–C2–C3–N1	C2–C3–N1–C4	C3–N1–C4–C9	N1–C4–C9–S1	C4–C9–S1–C1
dil	-27.8(2)	-55.6(2)	83.6(2)	1.4(3)	-49.8(4)	-7.8(3)	66.8(2)
dil-asa	-32.8(3)	-51.5(4)	84.3(5)	-0.8(6)	-51.8(6)	-5.4(6)	68.5(4)
dil-nia	-39.9(2)	-45.0(3)	89.9(3)	-10.1(3)	-48.7(3)	-1.7(3)	70.4(2)
dil-mal	-41.0(4)	-42.9(5)	90.7(5)	-13.7(7)	-46.0(7)	-1.9(7)	70.8(4)

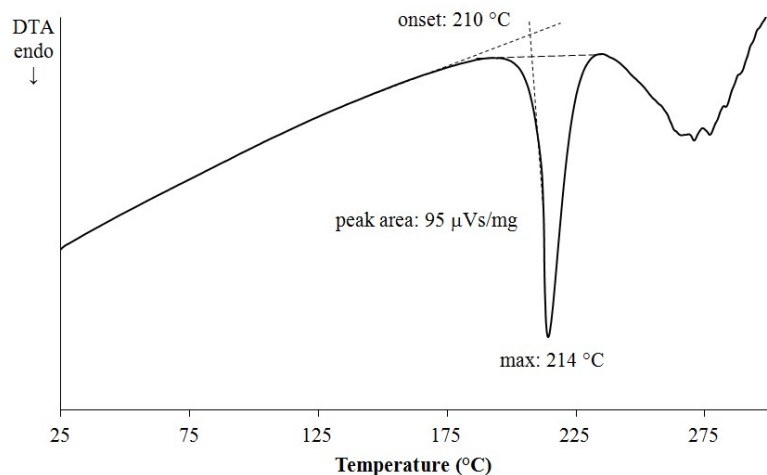


Fig. S13. DTA curve showing thermal properties of **dil**-HCl

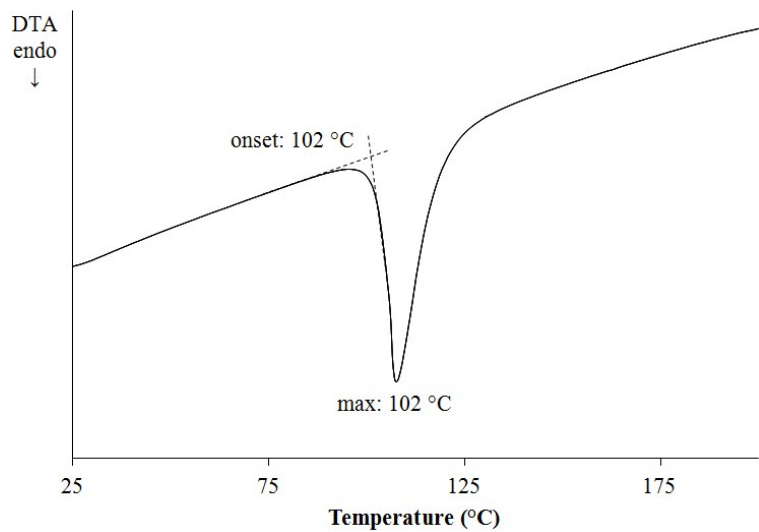


Fig. S14. DTA curve showing thermal properties of **dil**

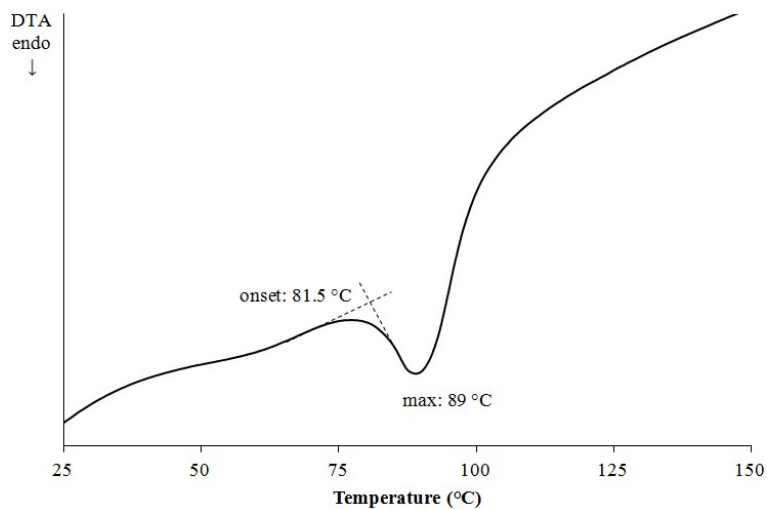


Fig. S15. DTA curve showing thermal properties of **dil-asa**

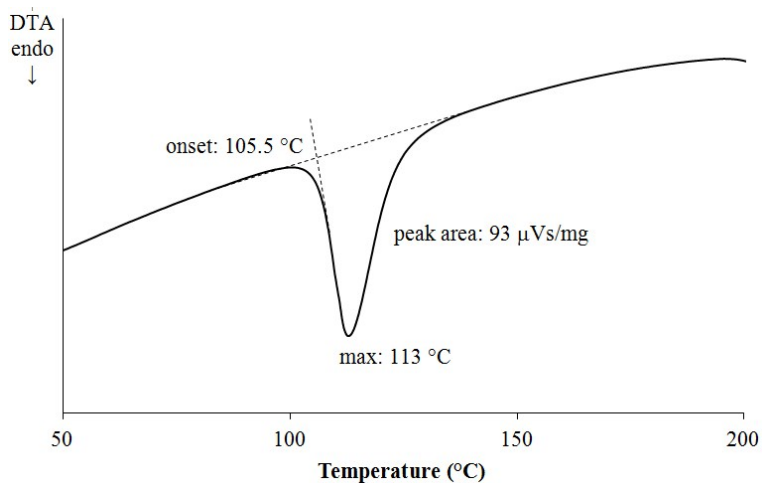


Fig. S16. DTA curve showing thermal properties of **dil-nia**

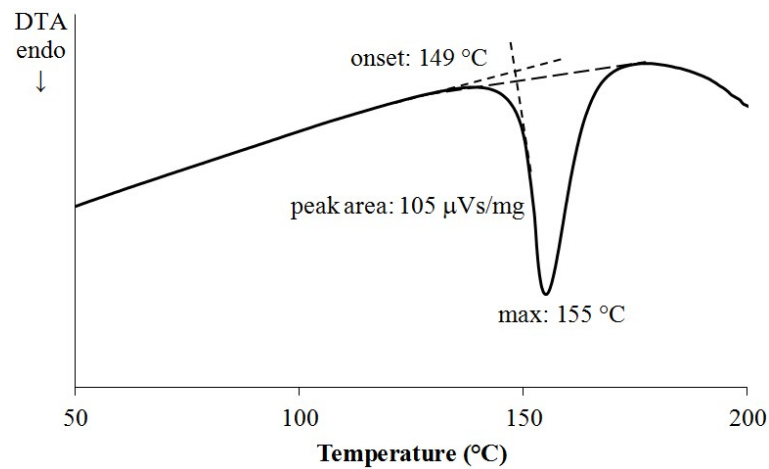


Fig. S17. DTA curve showing thermal properties of **dil-mal**

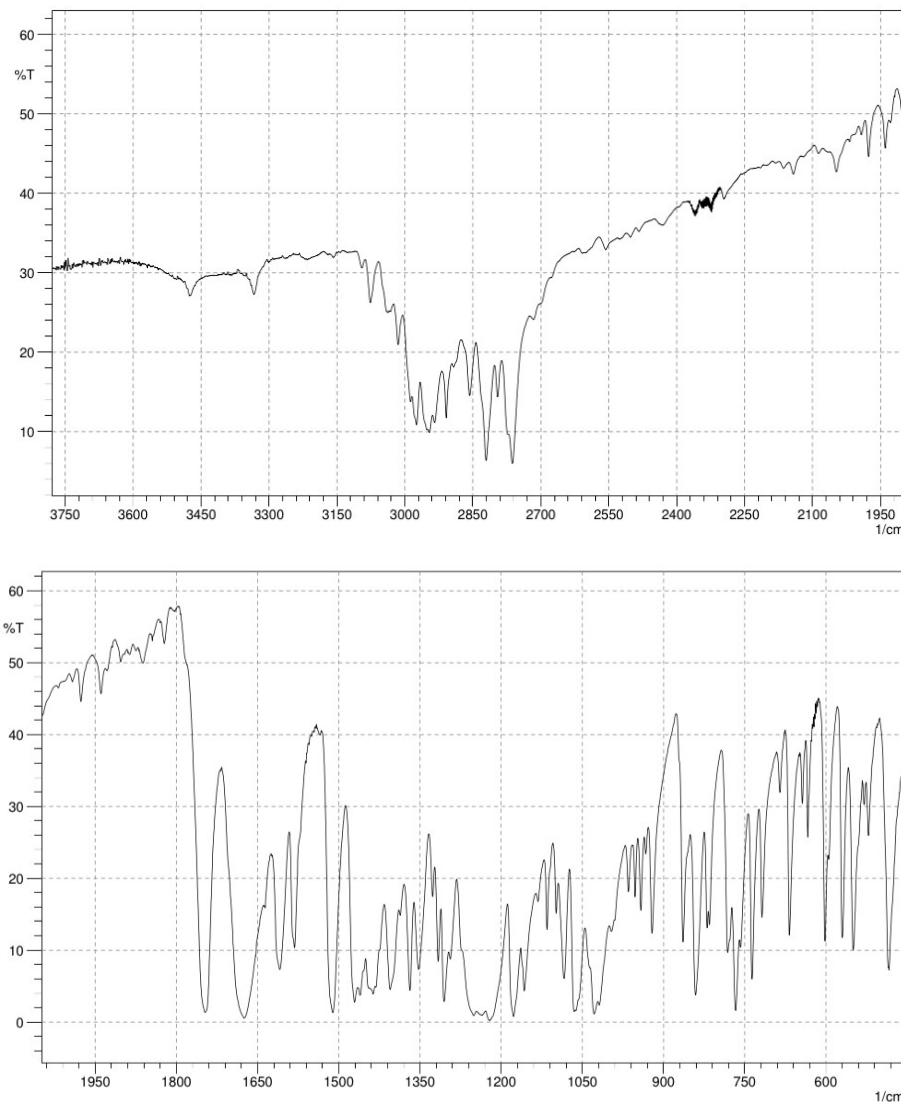


Fig. S18. FT-IR of **dil**

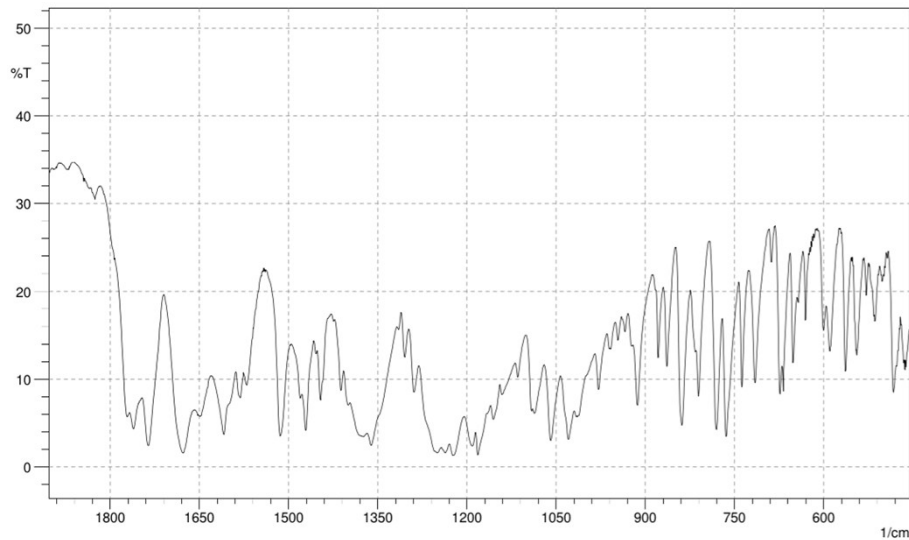
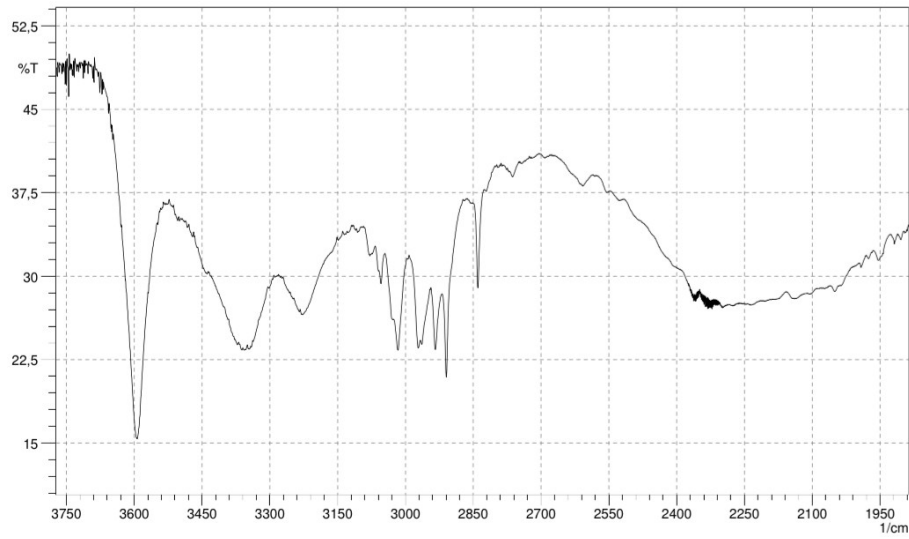


Fig. S19. FT-IR of **dil-asa**

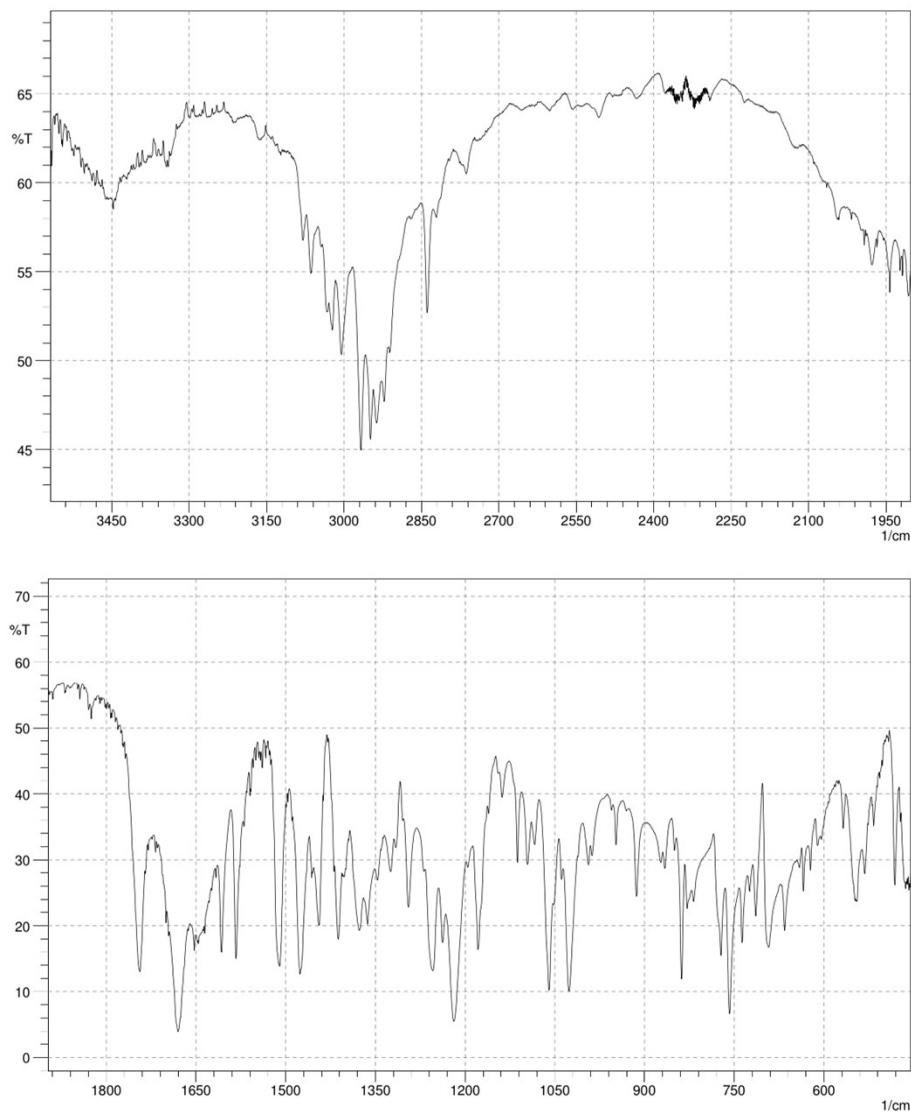


Fig. S20. FT-IR of **dil-nia**

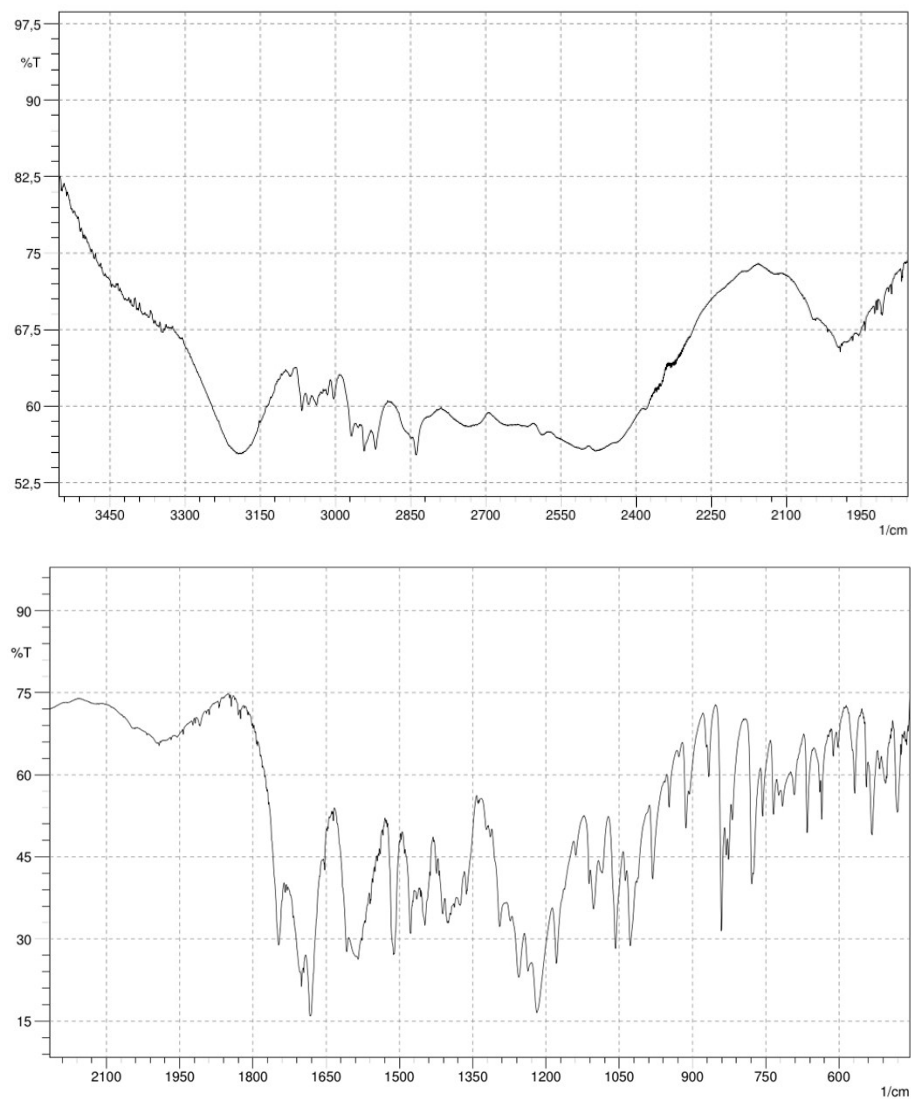


Fig. S21. FT-IR of **dil-mal**